Property−Structure Relationship of Nanoscale Ionic Materials Based on Multiwalled Carbon Nanotubes

Qi Li, Lijie Dong, Jingfei Fang, and Chuanxi Xiong*

State Key Laboratory of Advanced Technology for Materials Synthesis and Processing, and School of Materials Science and Engineering, Wuhan University of Technology, Wuhan 430070, China

ABSTRACT Two categories of nanoscale ionic materials (NIMs) based on multiwalled carbon nanotubes (MWCNTs) were obtained. According to the nature of organic modifier and the type of interaction, these NIMs can be divided into two categories referred to as A-MWCNTs-Fs and I-MWCNTs-Fs, respectively. These MWCNT derivatives were virtually solvent-free and showed good flowability even at room temperature. The liquidlike manner of these MWCNT derivatives was from their relatively high organic content and continual departing−recombining motion of the large organic ions as suggested by the comparison of rheological response of the two categories of MWCNT-based NIMs. Thermal property and temperature-dependent and strain-dependent viscoelasticity of MWCNT derivatives were related to the microscopic structure of their coating layer and subsequently related to the configuration, chemistry, and molecular dimension of modifying molecules to establish the property−structure relationship of MWCNT-based NIMs, which could guide our future work on NIMs to appropriate and promising applications based on their tunable and controllable physical properties.

KEYWORDS: carbon nanotubes · ionic materials · solvent-free · rheological property · structure

Surface functionalization of carbon nanotubes (CNTs) is necessary both for the modification of their chemical and physical properties and the acquirement of new characteristics. To make full utility of the excellent electrical, mechanical and thermal properties of CNTs and to realize full potential of CNT-based nanocomposites, plenty of research works have focused on their functionalization with the aim of enhancing solubility, preventing aggregation, and improving compatibility with polymers.[1−12]

Among the most recent research advances in the field of surface-functionalized nanostructures, nanoscale ionic materials (NIMs) pioneered by Giannelis and coworkers occupy a unique position due to their tailored physical properties which can span the spectrum from glassy-solid-like to Newtonian-liquid-like.[13−18] This unexpected nature originates from the inherent structure of their building blocks, each of which comprises a rigid nanoparticle core and a soft organic shell, where the shell is typically fabricated by grafting flexible charged organic oligomers to the surface of nanostructures.[19,20] Since the organic modifiers are covalently grafted to the nanoparticle surface and the core−shell structure can remain stable under physical disturbing, the whole system is regarded as single-component and macroscopically homogeneous.[21] By controlling the grafting density and chemical characteristics of organic moiety or core particle chemistry in the synthesis of NIMs, a zero-vapor-pressure liquidlike product can be obtained.[15] Unlike conventional colloidal suspension systems, in which solvents have to be employed to dissolve or suspend nanoparticles, these liquidlike NIMs are completely solvent-free. Therefore, these NIMs are also referred to as solvent-free nanofluids or self-suspended nanoparticles.[22]

To date, several research groups have reported NIMs based on mutiwalled carbon nanotubes (MWCNTs).[19,23,24] In general, these MWCNT-based NIMs can be roughly divided into two categories according to the nature of organic modifier and the type of interaction. In the first category the MWCNT derivatives are synthesized via an acid−base reaction or hydrogen bonding between the surface −OH or C═O groups of MWCNTs and the amine groups of organic modifiers,[23,24] whereas the derivatives in the second category are prepared *via* electrostatic combination of two oppositely charged organic ions, one of which is previously grafted to the end-caps or side walls of MWCNTs.[19] These works mainly focused on the preparation and characterization of MWCNT-based NIMs. However, reports concerning the relationship between the

*Address correspondence to cxx@live.whut.edu.cn.

Received for review July 7, 2010 and accepted August 31, 2010.

Published online September 3, 2010. 10.1021/nn101542v

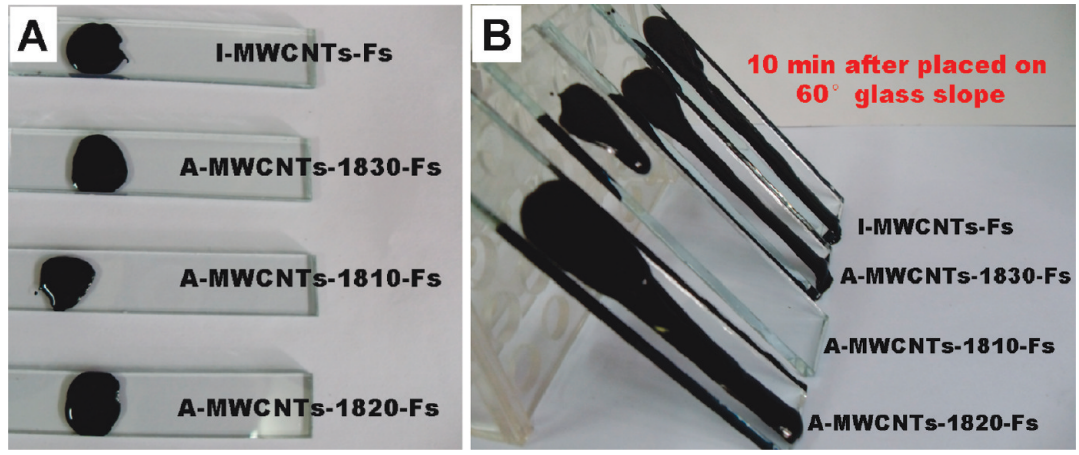

Figure 1. Photographs of MWCNT-based NIMs (A) placed on glass slides and (B) flowing down 60° glass slopes.

output rheological properties and microscopic structures of MWCNT-based NIMs or the difference between the above-mentioned two categories are rare.

In this work, by employing appropriate organic modifiers, two categories of MWCNT-based NIMs within the liquidlike region are prepared and termed A-MWCNT-Fs (solvent-free MWCNT fluids synthesized *via* acid−base reaction process) and I-MWCNT-Fs (solvent-free MWCNT fluids synthesized *via* ion-exchange process), respectively. Effects of organic modifiers on structure and rheological properties are evaluated by introducing poly(ethylene) glycol (PEG)-substituted tertiary amines with diverse molecular weights to the NIM systems. Rheological responses of both the two categories of MWCNT-based NIMs are related to their microscopic structures to tell the differences stemming from the nature of organic modifiers and to explore the essence of their especial rheological property. The findings reported here can provide fundamental data about the structure control of MWCNT-based NIMs, and their output properties determined by structure can also be tuned according to the property−structure relationship. Moreover, the establishment of property−structure relationship may largely expand and correctly direct the application of MWCNT-based NIMs, especially those with self-suspending capability on account of the great significance of suspensions in the preparation of many types of materials.

RESULTS AND DISCUSSION

Carboxylic MWCNTs are converted to the oxidized form by a sonication-assisted oxidation in concentrated acids before use, in order to shorten their length and increase the population density of surface hydrophilic groups. I-MWCNTs-Fs are prepared through a two-step procedure. First, oxidized MWCNTs are covalently grafted with a charged polysiloxane quaternary ammonium salt (DC5700) $[(CH_3O)_3Si(CH_2)_3N^+(CH_3)_2(C_{18}H_{37})Cl^-]$ to render them cationic,[19] which then react with a PEG-functionalized sulfonate salt $[C_9H_{19}-C_6H_4-O(CH_2CH_2O)_{10}SO_3^-K^+]$ to allow for an ion exchange.[16] The preparation strategy of A-MWCNTs-Fs follows a reported protocol,[23] with some small changes. Depending on the PEG-substituted tertiary amines $(C_{18}H_{37})N[(CH_2CH_2O)_mH][(CH_2CH_2O)_nH]$ used during the preparation, which are known as 18/10, 18/20, and 18/30 ($m + n$ = 10, 20, and 30), respectively, three types of A-MWCNTs-Fs are prepared, denoted as A-MWCNTs-1810-Fs, A-MWCNTs-1820-Fs, and A-MWCNTs-1830-Fs.

As shown in Figure 1A, each type of the as-prepared MWCNT-based NIMs (0.3 g) is placed on an individual glass slide (10 cm ×1.5 cm size) at room temperature (25 °C), and they all appear as a liquid without any heating. To exhibit their flowability, we raised one end of each glass slide to convert them to 60° glass slopes. The flowing behavior of these MWCNT derivatives driven by gravity can be observed immediately, and after 10 min, only A-MWCNTs-1810-Fs failed to reach to the bottom of slope owing to its relatively high viscosity (Figure 1B).

To evaluate the results of sonication-assisted oxidization in concentrated acids, Fourier transformation infrared (FTIR), Raman, and transmission electron microscopy (TEM) measurements are investigated. The FTIR results are shown in Figure 2A. Compared to original carboxylic MWCNTs, the oxidized MWCNTs exhibit stronger bands at 3417, 1711, and 1172 cm^{-1}, which can be assigned to the O−H stretching vibrations of −OH groups, C═O stretching vibrations of −COOH groups, and C−O stretching vibrations of C−OH, respectively, indicating that more hydroxyl and carboxylic acid groups are introduced to their end-caps and side walls. Another evidence for the increase of surface reactive groups of MWCNTs comes from the Raman spectrum shown in Figure 2B. The D (disorder mode) band at 1347 cm^{-1} corresponds to sp^3-hybridized carbons, while the G (graphite) band at 1584 cm^{-1} is attributed to sp^2-hybridized carbons. The intensity ratio of D band and G band I_D/I_G increases from 0.588 to 0.839

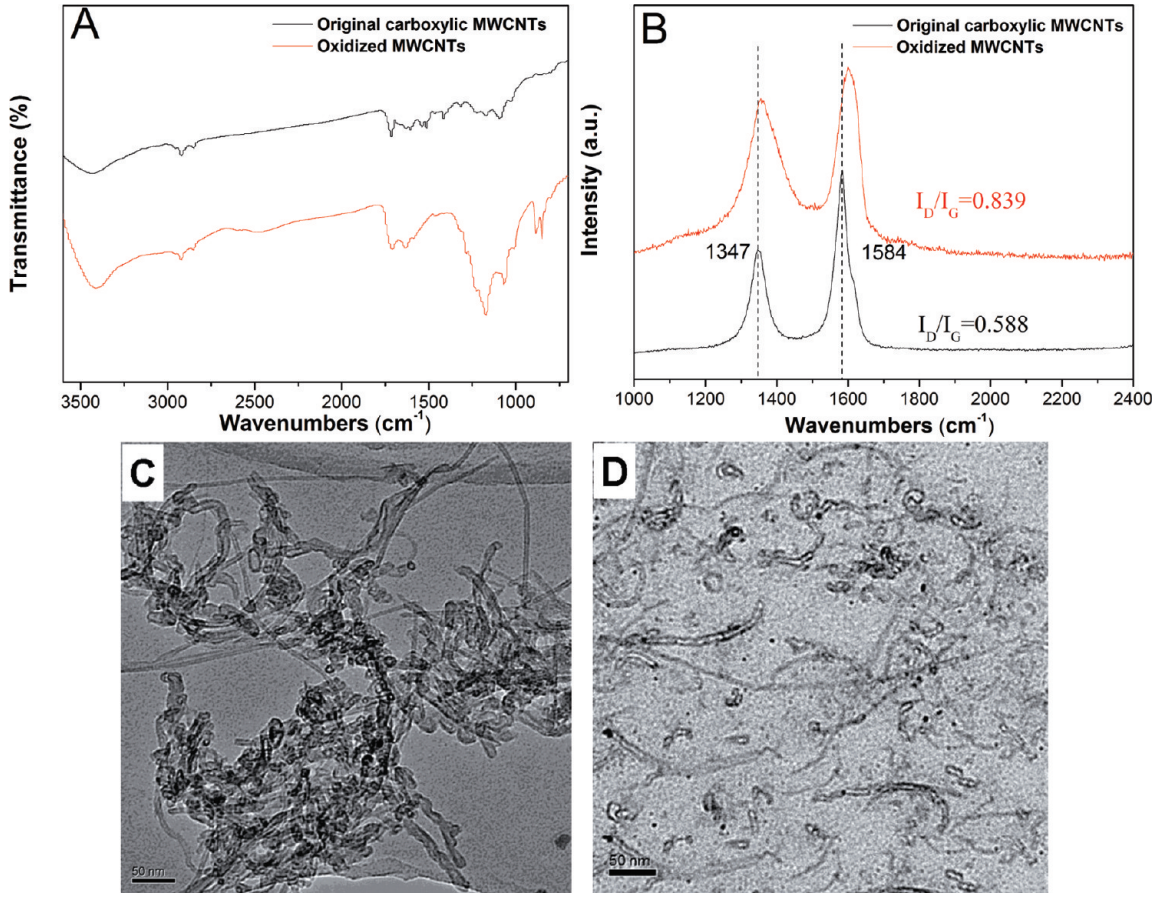

Figure 2. (A) FTIR spectra of original carboxylic MWCNTs and oxidized MWCNTs. (B) Raman spectra of original carboxylic MWCNTs and oxidized MWCNTs. TEM images (scale bar: 50 nm) of (C) original carboxylic MWCNTs and (D) A-MWCNTs-1830-Fs.

after the oxidization, characteristic of more surface functional groups. It can also be seen from TEM images in Figure 2C and D that the long original carboxylic MWCNTs (10−30 μm length) are highly entangled with each other, which are then cut into shorter forms through an oxidation by concentrated acids with a concomitant sonication, and in the final product, they show untangled appearance with an average length of about 100 nm.

Although the as-received MWCNTs contain surface carboxyl groups, they show bad solubility both in aqueous and organic solvents (chloroform) due to their ultralong dimensions (Figure 3, column 1) and strong van der Waals interactions that hold them together. After an oxidation and sonication, the long MWCNTs are cut into shorter forms and more polar hydrophilic groups are introduced to their surfaces. As a result, these oxidized MWCNTs can be dispersible in water (Figure 3, column 2, upper part) but still aggregate heavily in organic solvent (Figure 3, column 2, lower part). In sharp contrast, all the MWCNT derivatives are amphiphilic as indicated by their perfect solubility in aqueous/organic solvents (Figure 3, columns 3−6), which is a result of their ionic nature as well as the presence of PEG chain segments.[23]

FTIR is also applied to verify the surface functionalization of MWCNTs. Figure 4A shows the FTIR spectra of oxidized MWCNTs, DC5700-grafted MWCNTs, and I-MWCNTs-Fs. The peaks at 2921, 2853, 1466, and 1113 cm^{-1} in the spectrum of DC5700-grafted MWCNTs correspond to C−H stretching vibrations of $-CH_3$, C−H stretching vibrations of $-CH_2-$, in-plane bending vibrations of $-CH_2-$, and C−O−Si stretching vibrations, respectively, indicating the grafting of DC5700. In the

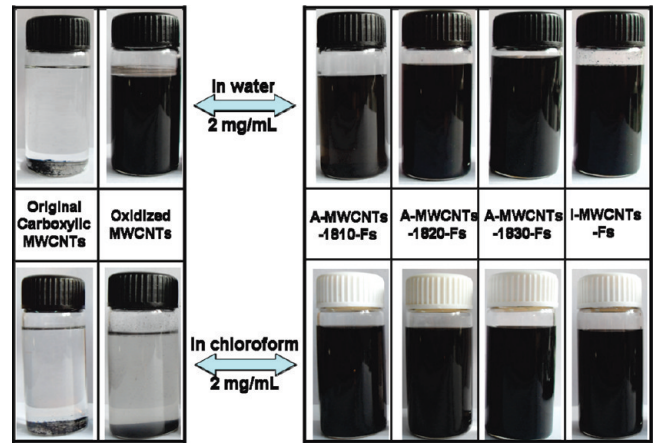

Figure 3. Solubility of original carboxylic MWCNTs, oxidized MWCNTs, and MWCNT derivatives.

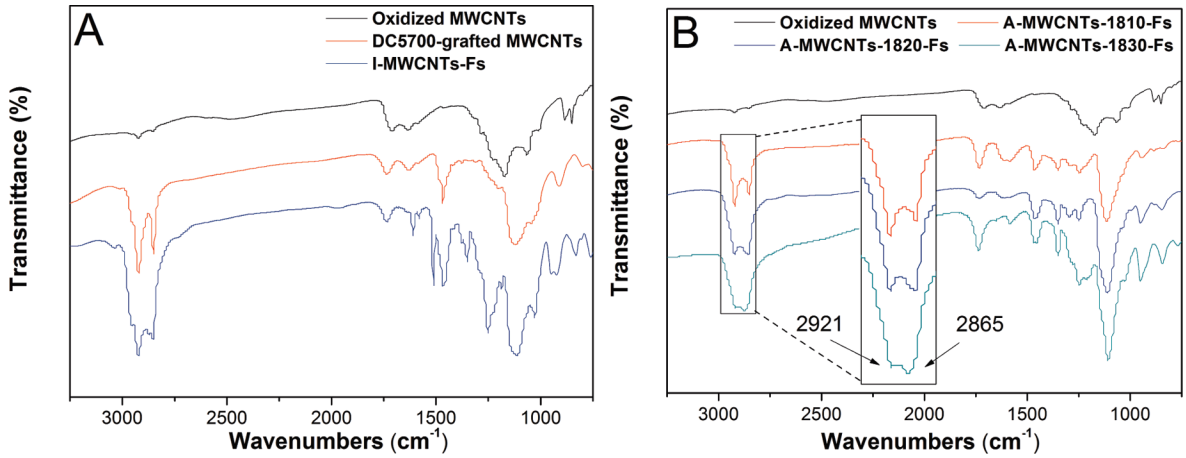

Figure 4. (A) FTIR spectra of oxidized MWCNTs, DC5700-grafted MWCNTs, and I-MWCNTs-Fs. (B) FTIR spectra of oxidized MWCNTs and the three types of A-MWCNTs-Fs.

spectrum of I-MWCNTs-Fs, ionic exchange by PEG-functionalized sulfonate ion is confirmed by the presence of benzene skeleton vibration at 1610 and 1512, and $-SO_3^-$ absorption band at 1250 cm^{-1}. As shown in Figure 4B, C−H stretching vibrations of $-CH_3$ at ~2920 cm^{-1}, C−H stretching vibrations of $-CH_2-$ at ~2860 cm^{-1}, and C−O−C stretching vibrations at ~1110 cm^{-1} in the FTIR spectra of the three types of A-MWCNTs-Fs (A-MWCNTs-1810-Fs, A-MWCNTs-1820-Fs and A-MWCNTs-1830-Fs) indicate that PEG-substituted tertiary amines are successfully reacted with oxidized MWCNTs. The amplified region in Figure 4B illustrates the detailed information about the decreasing methyl/methylene ratio, demonstrating the increasing length of PEG chain in tertiary amine molecules.

Thermogravimetric analysis (TGA) (Figure 5A) shows that all these MWCNT derivatives are virtually solvent-free as implied by zero weight loss within the low temperature range, and their organic contents are, as calculated from the weight loss up to 600 °C, 73%, 82%, 86%, and 82%, corresponding to A-MWCNTs-1810-Fs, A-MWCNTs-1820-Fs, A-MWCNTs-1830-Fs, and I-MWCNTs-Fs, respectively. Two factors should be responsible for such relatively high organic contents: (1) small diameter and shortened length of the oxidized nanotubes and (2) high grafting density of MWCNT derivatives. Remarkably, we find that the values of organic content are proportional to that of the molecular weight of corresponding modifying molecules. The grafting density is revealed by further calculation based on the TGA data as listed in Table 1. Obviously, all the data of grafting density are very close to a constant value, which is highly dependent on the population density of polar hydrophilic groups on the surface of oxidized MWCNTs. Since the molecular weight of these modifying molecules differs from each other and all the MWCNTs are treated at the same conditions in the oxidization process, this invariable grafting density implies that there is almost a stable modifying molecule/surface reactive group stoichiometry in the MWCNT derivatives, which also means there is no excess modifying molecules but chemically bonded ones existing in the MWCNT derivatives. Therefore, the organic content of these MWCNT-based NIMs can be tuned by simply employing modifying molecules with diverse molecular weight.

As indicated by differential thermogravimetric (DTG) traces in Figure 5B, MWCNTs functionalized by organic modifiers with larger alkyl chain fraction bear a higher weight loss around 300 °C, while those modified by organic molecules with larger PEG chain fraction lose their majority of weight at about 400 °C. Considering that a carbon−oxygen bond has a higher bond energy compared with a carbon−carbon bond, we suspect that the weight loss at about 300 and 400 °C are attributed to the deformation of alkyl and PEG chain segment, respectively. Therefore, it can be concluded that higher thermal stability can be achieved by employing modifying molecules with larger PEG chain fraction in a NIM system.

Differential scanning calorimetry (DSC) results exhibited in Figure 5C reveal that all these MWCNT-based NIMs can melt reversibly and the melting and crystallizing temperatures highly depend on the nature of modifying molecules. Namely, NIMs modified by organic molecules with low melting point possess low solid-to-liquid transition temperature. Although phase transition temperature has no direct relation with organic content in a NIM system judging from the DSC profiles, the enthalpy of melting is intimately linked to the proportion of organic fraction.

Liquidlike behavior of all the as-prepared I-MWCNTs-Fs and A-MWCNTs-Fs is confirmed by the higher loss modulus (G′′) compared with storage (G′) modulus in the temperature-dependent G′ and G′′ measurements at fixed angular frequency (ω) and strain amplitude (γ), as shown in Figure 6A,B.[13] Normally, modulus (Figure 6A,B) and viscosity (Figure 6C) of all the samples decrease with increasing temperature, and A-MWCNTs-Fs with higher organic content have lower

TABLE 1. Grafting Density of the MWCNT-Based NIMs

organic moiety	molecular weight of organic moiety	organic content of corresponding NIMs (%)	grafting density (number of modifying molecule per carbon atom)
18/10	~709	73	~22
18/20	~1149	82	~21
18/30	~1589	86	~22
DC5700 and the sulfonate	~1180 (paired cation and anion)	82	~21

modulus and viscosity at the same temperature. Remarkably, although A-MWCNTs-1820-Fs possess the same organic content (82%) to I-MWCNTs-Fs, they are more viscous as indicated by their higher modulus (Figure 6B) and viscosity (Figure 6C) value, and as the temperature increases, the viscosity of I-MWCNTs-Fs decreases much faster than that of A-MWCNTs-Fs. This detail opens a way to understand the difference of the two categories of MWCNT-based NIMs. It is known that the interactions between ion pairs are dominated by Coulombic force and the ions here are not simply spheres of charge but have shape. The paired cation and anion are ionicly combined with each other in the MWCNT-based NIMs and at their molten state within the testing temperature range in the rheological measurements. Therefore, with increasing temperature, charge centers of paired cation and anion can move apart to a certain distance or even recombine with other ions nearby, and this effect can cause the continual departing−recombining motion of large organic ions that favors smooth slipping between the adjacent building blocks and subsequently the flowability of corresponding bulky material. For I-MWCNTs-Fs, PEG-functionalized sulfonate anions are all ionicly combined with DC5700 cations, so the above-mentioned effect can yield great benefits to the fluidity of this sample. Nevertheless, for A-MWCNTs-1820-Fs, that effect is restricted by two factors: (1) the ion pair of quaternary ammonium cation and carboxylate anion formed by ionicly grafting of PEG-substituted tertiary amines to the surface of MWCNTs cannot be apart as allodially as the pair of DC5700 cation and the sulfonate anion at the same temperature; (2) part of PEG-substituted tertiary amines are grafted to the surface of MWCNTs through hydrogen bonding to the surface −OH or C═O groups by amine groups. Consequently, A-MWCNTs-Fs are more viscous than I-MWCNTs-Fs at the same conditions. The difference between the two categories of MWCNT-based NIMs in the nature of organic modifier and the type of interaction makes them dissimilar in rheological response. Concluded from the above-discussed rheological properties, the NIMs behave as liquid due primarily to the continual departing−recombining motion of the large organic ions from room-temperature molten ion pairs which can also be denoted as room-temperature molten salts.

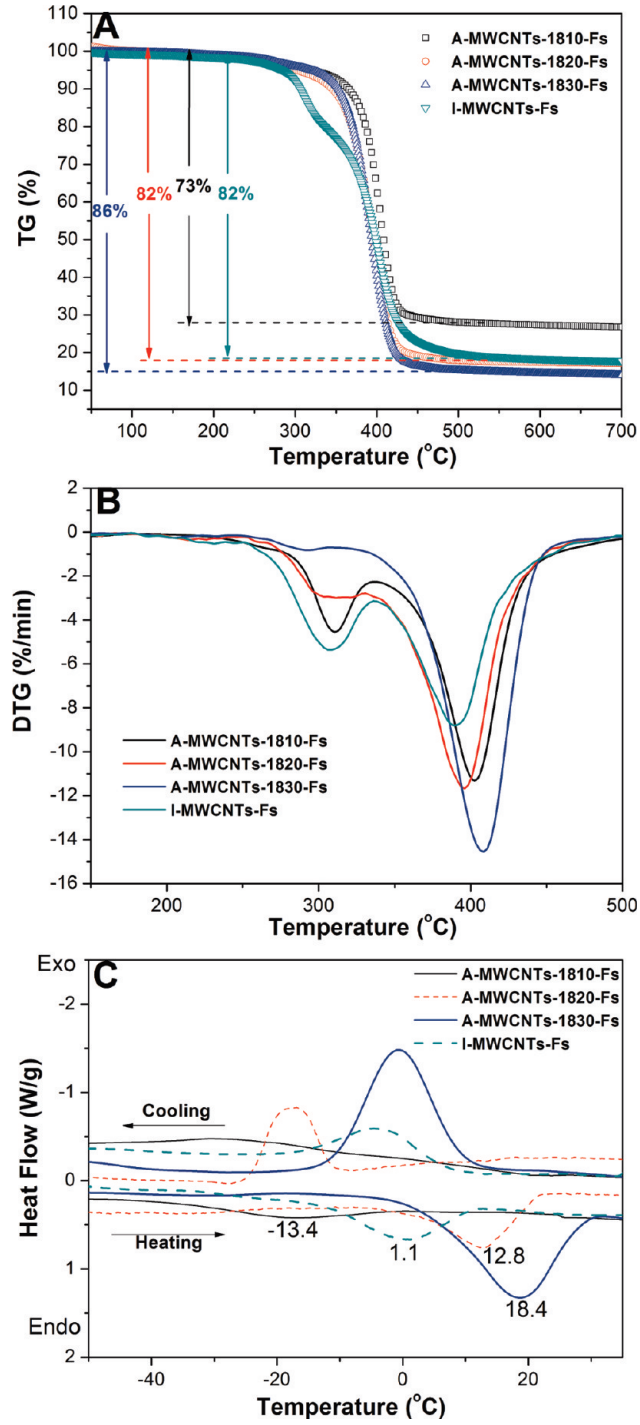

Figure 5. (A) TGA traces, (B) DTG traces, and (C) DSC profiles of I-MWCNTs-Fs and the three types of A-MWCNTs-Fs.

High-resolution transmission electron microscopy (HRTEM) measurement can give direct characterization of microscopic structure and thus supply an opportunity to understand the essence of output properties. In this section, HRTEM images of original carboxyl MWCNTs, oxidized MWCNTs, and MWCNT derivatives are investigated. Figure 7A shows a HRTEM image of original carboxyl MWCNTs. It can be seen clearly that the diameter of every single nanotube is smaller than 8 nm and the side wall is uniformly flat with ordered

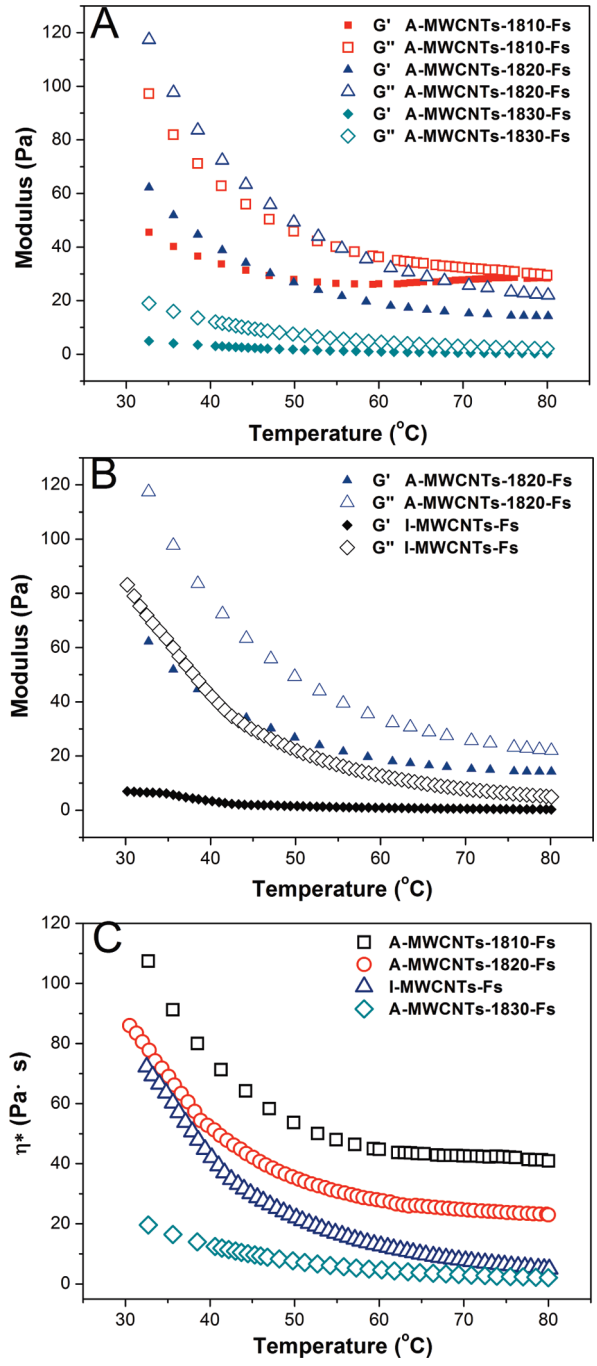

Figure 6. Temperature-dependent modulus of (A) the three types of A-MWCNTs-Fs and (B) I-MWCNTs-Fs and A-MWCNTs-1820-Fs. (C) Viscosity−temperature traces of I-MWCNTs-Fs and the three types of A-MWCNTs-Fs.

crystal lattice extending to the edge. Although the HR-TEM image of oxidized MWCNTs (Figure 7B) shows some defects at fringes of the nanotubes, the crystal lattice is still obvious even to the outmost part of the side wall.

In contrast, as shown in all the HRTEM images of the MWCNT derivatives (Figure 7C−F), MWCNTs are densely grafted with organic chains as indicated by the coating shell structure void of any crystal lattice. As the molecular chain length of organic modifiers in each type of MWCNT derivative increases, the shell thickness changes accordingly, and the measured values of shell thickness estimated from TEM images are shown in Table 2. By summing up all the bond lengths with bond angles taken into account, the full length of chain segment from grafting site to the terminal atom can be calculated, and the values are also listed in Table 2 as a comparison. The organic shell thickness here is highly dependent on three factors: (1) whether the organic chains are perpendicular to the nanotube surface, (2) whether the organic chains are stretched to their full length without curving, and (3) how much the paired cation and anion are apart from each other. The PEG-substituted tertiary amines are terminated with very flexible PEG chain segments, which readily results in chain curving, and longer PEG-chain-substituted tertiary amines can cause higher curving degree. Besides, the quaternary ammonium cation and carboxylate anion can only be apart to a relatively short distance. Therefore, the measured value of organic shell thickness for every type of A-MWCNTs-Fs is lower than the full length of chain segment to different extents.

TABLE 2. Organic Shell Thickness of the MWCNT-Based NIMs

organic moiety	chain length from grafting site to the terminal atom (nm)	estimated value from TEM image (nm)
18/10	~2.1	~2
18/20	~3.6	~2.5
18/30	~5.1	~3
DC5700 and the sulfonate	~6	~6

For I-MWCNTs-Fs, it has been verified by our previous work that DC5700 and the PEG-functionalized sulfonate anion can form a perpendicular bilayer structure on the nanostructure surface,[19,20] and although the molecular chain of grafted modifier is rather long compared with every single PEG chain of the PEG-substituted tertiary amines, the bilayer structure is ended with alkyl chain segment that is less flexible than the PEG chain and contains a rigid benzene structure. As a result, at such high grafting density, there are a larger proportion of stretched chains approximately perpendicular to the nanotube surface. Additionally, at the molten state, the sulfonate anion can move farther from the quaternary ammonium cation than carboxylate anion. Consequently, the measured value of the organic shell thickness for I-MWCNTs-Fs is very close to the calculated value of the full length of chain segment. Obviously, the two categories of MWCNT-based NIMs have analogous organic−inorganic core−shell structures but differ from each other in modifying molecule arrangement, which not only affects their microscopic morphology but also has an influence on their rheological property.

Figure 8 panels A and B show the shear strain-dependent modulus of A-MWCNTs-1820-Fs and

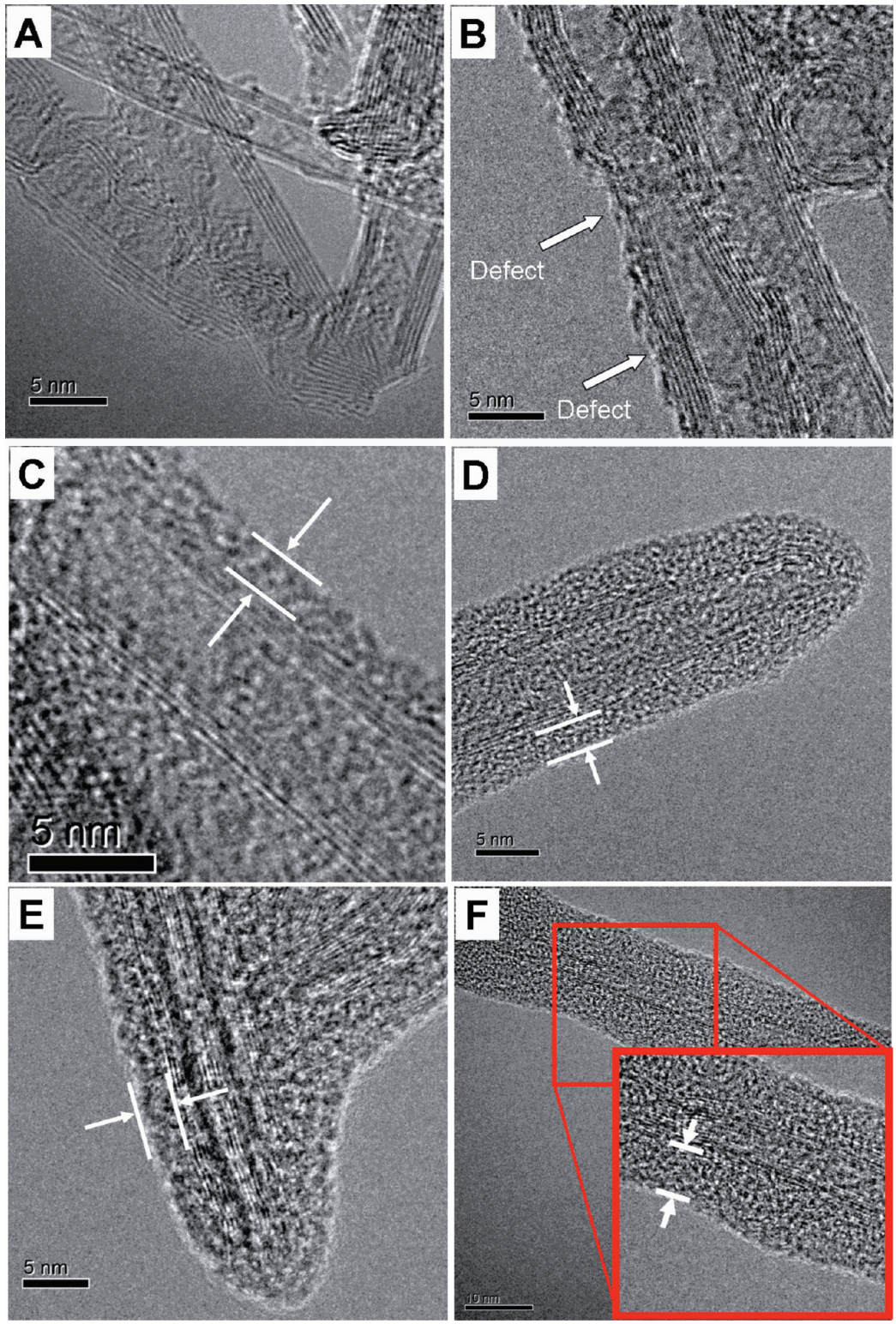

Figure 7. HRTEM images of (A) original carboxylic MWCNTs, (B) oxidized MWCNTs, (C) A-MWCNTs-1810-Fs, (D) A-MWCNTs-1820-Fs, (E) A-MWCNTs-1830-Fs, and (F) I-MWCNTs-Fs.

I-MWCNTs-Fs. The G′ of both samples maintains stable at low shear strain and begins to decay at a critical strain amplitude of about 2% which is also known as the yield strain. In contrast, although the G′′ plots of A-MWCNTs-1820-Fs and I-MWCNTs-Fs have analogical trends, there is a pronounced peak in the G′′ plot of I-MWCNTs-Fs near the critical strain value, while that of A-MWCNTs-1820-Fs is void of this characteristic. By referring to the previous literatures we know that the peak in G′′ plot is a typical feature of soft glassy materials where the constitutive elements are trapped in tight cages from which they cannot spontaneously es-

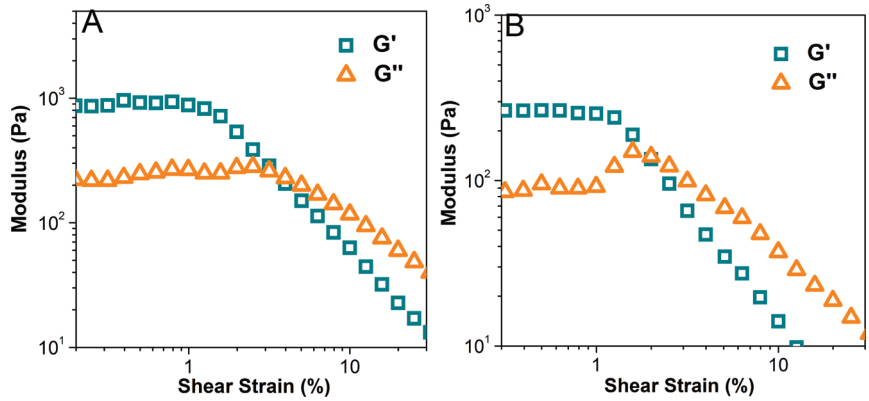

Figure 8. Strain-dependent modulus of (A) A-MWCNTs-1820-Fs and (B) I-MWCNTs-Fs.

cape, and these cages are in fact formed by their adjacent constitutive elements.[25−28] As described by the proposed model of soft glassy materials, at their solid regime, the constitutive elements are restricted within a very limited room by repulsive interactions between adjacent neighbors. Once the cage distortion by shear allows for particle rearrangements, the system begins to behave as liquid.[29,30] In the strain-dependent modulus plot of I-MWCNTs-Fs (Figure 8B), the solidlike region is suggested by higher G′ compared with G′′, and at this phase, the modifying molecules are entangled with each other to play a role of fastening the cage. The decay of G′ occurs at the yield strain, and the appearance of a maximum in G′′ indicates that the mechanical energy is dissipated when the cage breaks apart. Meanwhile, the G′ plot intersects with that of G′′, denoting the beginning of the liquidlike region. In this region, due to the sharply weakened repulsive interactions between adjacent constitutive elements and the speeding up of structural relaxation caused by increased shear strain, the building blocks can move much more freely and the motion of modifying molecules becomes active, and thus they play a role of lubricant or even fluidization medium. The NIMs can show soft glassy rheology only when the dimension of core structure is comparable to the thickness of coating layer and the grafting density is high enough to ensure the small spacing of modifying molecular chains.[22] It is at this situation that the modifying molecule can exhibit rodlike conformation and be coupled with core structure motions. The building blocks of A-MWCNTs-1820-Fs possess a coating layer of only 2.5 nm in thickness that consists of highly curved organic molecules and are not thick enough for them to fill the intervening space between the core structures. In contrast, I-MWCNTs-Fs with a 6 nm thick organic shell consisted of stretched organic molecules in accord with the above-mentioned preconditions very well, and as a result, they show soft glassy properties. It is well-known that the mechanical properties of nanoparticle-filled polymer composite can be promoted by obtaining well dispersed large volume fractions of the reinforcing nanoparticles and realizing an effective load transfer from the polymeric matrix to the reinforcing nanoparticles.[31] NIMs with soft glassy rheology are promising alternative to these filling nanoparticles owing to the underlying two factors of (1) self-suspending nature and (2) coupled modifying molecule and core structure motions. Factor 1 is of great value for processability, manipulation, and ease of dispersion, while factor 2 favors load transfer from polymeric matrix to nanostructures given that the modifying molecules have good compatibility with the matrix.

In summary, a new class of chemically functionalized MWCNTs termed MWCNT-based NIMs have been synthesized, where uniform core−shell structured MWCNT derivatives with different shell thickness can be obtained by simply varying the modifying molecules, and these solvent-free MWCNT derivatives show good flowability even at room temperature. According to the nature of organic modifier and the type of interaction, these NIMs can be divided into two categories referred to as A-MWCNTs-Fs and I-MWCNTs-Fs, respectively. The findings reported here can provide fundamental data about the structure control of MWCNT-based NIMs, and the comparison of rheological response between the two categories of MWCNT-based NIMs opens a way to understand the essence of their unique liquidlike manner. By investigating the output properties and microscopic structures, we discuss their property−structure relationship, especially how the structure determines the peculiar rheological response. The established property−structure relationship may guide our future work on NIMs to appropriate and promising applications based on their tunable and controllable physical properties.

EXPERIMENTAL SECTION

Materials and Preparation. Carboxylic MWCNTs (chemical vapor deposition method; diameter, <8 nm; length, 10−30 μm; purity, ≥95%) were purchased from Chengdu Organic Chemicals Co., Ltd., Chinese Academy of Sciences. Polysiloxane quaternary ammonium salt DC5700 $[(CH_3O)_3Si(CH_2)_3N^+(CH_3)_2(C_{18}H_{37})Cl^-]$ in methanol (40%) was provided by Gelest. PEG-functionalized sulfonate salt $C_9H_{19}-C_6H_4-O(CH_2CH_2O)_{10}SO_3^-K^+$ was from Aldrich.

PEG-substituted tertiary amines ($C_{18}H_{37}$)N[(CH_2CH_2O)$_m$H][(CH_2CH_2O)$_n$H], known as 18/10, 18/20, and 18/30 ($m + n$ = 10, 20, and 30), were received from Azko-Nobel. Anhydrous methanol (AR), anhydrous ethanol (AR), H_2SO_4 (98%), HNO_3 (65%), and chloroform (AR) were all from Sinopharm Chemical Reagent Co., Ltd., China.

Typically, carboxylic MWCNTs were sonicated in 1:3 concentrated nitric acid−sulfuric acid at 50 °C for 5 h. The dispersion was then centrifuged and the remaining solid was washed repeatedly with deionized water before the pH value of its aqueous solution (1% wt./vol.) was 3. I-MWCNTs-Fs were prepared through a two-step procedure. First, the as-prepared aqueous solution of oxidized MWCNTs (50 mL, pH 3) was added into DC5700 (40%, 5 mL) to render them cationic. The mixture was then sonicated for 2 h, washed 3 times with deionized water and twice with anhydrous ethanol, and dried at 70 °C. Second, DC5700-grafted MWCNTs and 1.5 g PEG-functionalized sulfonate salt were dissolved by 50 mL of chloroform, and the solution was added into a three-neck flask and stirred for 5 h at room temperature. Subsequently, 20 mL of deionized water was added into the solution to remove the KCl salt and excess PEG-functionalized sulfonate salt, and the reaction was stirred for another 2 h. The upper layer was removed by pipet, and more deionized water was added into the flask. After stirring 2 h, the water was again removed. This was repeated for 3 times before the lower layer was collected and dried at room temperature. The preparation strategy of A-MWCNTs-Fs followed a reported protocol, with some small changes. The pH value of as-prepared aqueous solution of oxidized MWCNTs (50 mL) was adjusted to 7 by the dropwise addition of a 10% wt/vol aqueous solution of the PEG-substituted tertiary amine 18/10 (or 18/20, 18/30) and the mixture was dried at 70 °C. The resulting material was washed three times with toluene and twice with anhydrous ethanol and then dialyzed using a cellulose dialysis membrane/bag (trapped molecular weight >8200) by circulating deionized water around the dialysis bag for 48 h to further remove excess tertiary amines and other impurities. Finally, the product was dried at 70 °C for 24 h.

Characterization. FTIR measurements were carried out on a FTIR spectrometer (Thermo Nicolet Nexus) using KBr pellets. The Raman spectrum was recorded with a laser confocal Raman microscope (Renishaw System, 532 nm, 2−3 mW). TGA and DTG were performed with a simultaneous thermal analyzer (Netzsch, STA 499C) under N_2 flow. DSC was collected on a Perkin-Elmer Pyris instrument (PE) at a heating or cooling rate of 10 °C/min. Rheological properties were studied using a strain-controlled rheometer (Rheometrics Fluids Spectrometer, ARES-RFS). The temperature−modulus trace was recorded at fixed angular frequency ω of 1 s^{-1} and strain amplitude of 10%, and the temperature range was 30−80 °C at a constant heating rate of 3 °C/min. In the strain-dependent storage and loss modulus testing, the angular frequency ω was 1 s^{-1}, the temperature was 30 °C, and the shear strain range was 0.1−100%. TEM images were obtained with a Joel JEM-2001F electron microscope and all the samples were prepared by dispersing the material in ethanol, placing a few drops of the dispersion on a copper grid, and evaporating them prior to observation.

Acknowledgment. This work was financially supported by Doctoral Fundation of Higher Education of China (No. 200804970002), the National Natural Science Foundation of China (No. 50802068), and Self-Determined and Innovative Research Funds of WUT.

REFERENCES AND NOTES

1. Chen, J.; Hamon, M. A.; Hu, H.; Chen, Y.; Rao, A. M.; Eklund, P. C.; Haddon, R. C. Solution Properties of Single-Walled Carbon Nanotubes. *Science* **1998**, *282*, 95–98.
2. O'Connell, M. J.; Bachilo, S. M.; Huffman, C. B.; Moore, V. C.; Strano, M. S.; Haroz, E. H.; Rialon, K. L.; Boul, P. J.; Noon, W. H.; Kittrell, C.; Ma, J. P.; Hauge, R. H.; Weisman, R. B.; Smalley, R. E. Band Gap Fluorescence from Individual Single-Walled Carbon Nanotubes. *Science* **2002**, *29*, 593–596.
3. Czerw, R.; Guo, Z.; Ajayan, P. M.; Sun, Y.-P.; Carroll, D. L. Organization of Polymers onto Carbon Nanotubes: A Route to Nanoscale Assembly. *Nano Lett.* **2001**, *1*, 423–427.
4. Huang, W.; Lin, Y.; Taylor, S.; Gaillard, J.; Rao, A. M.; Sun, Y.-P. Sonication-Assisted Functionalization and Solubilization of Carbon Nanotubes. *Nano Lett.* **2002**, *2*, 231–234.
5. Niyogi, S.; Hamon, M. A.; Hu, H.; Zhao, B.; Bhowmik, P.; Sen, R.; Itkis, M. E.; Haddon, R. C. Chemistry of Single-Walled Carbon Nanotubes. *Acc. Chem. Res.* **2002**, *35*, 1105–1113.
6. Georgakilas, V.; Kordatos, K.; Prato, M.; Guldi, D. M.; Holzinger, M.; Hirsch, A. Organic Functionalization of Carbon Nanotubes. *J. Am. Chem. Soc.* **2002**, *124*, 760–761.
7. Riggs, J. E.; Guo, Z.; Carroll, D. L.; Sun, Y.-P. Strong Luminescence of Solubilized Carbon Nanotubes. *J. Am. Chem. Soc.* **2000**, *122*, 5879–5880.
8. Han, J.; Kim, H.; Kim, D. Y.; Jo, S. M.; Jang, S. Y. Water-Soluble Polyelectrolyte-Grafted Multiwalled Carbon Nanotube Thin Films for Efficient Counter Electrode of Dye-Sensitized Solar Cells. *ACS Nano* **2010**, *4*, 3503–3509.
9. Holzinger, M.; Vostrowsky, O.; Hirsch, A.; Hennrich, F.; Kappes, M.; Weiss, R.; Jellen, F. Sidewall Functionalization of Carbon Nanotubes. *Angew. Chem., Int. Ed.* **2001**, *40*, 4002–4005.
10. Michelson, E. T.; Chiang, I. W.; Zimmerman, J. L.; Boul, P. J.; Lozano, J.; Liu, J.; Smalley, R. E.; Hauge, R. H.; Margrave, J. L. Solvation of Fluorinated Single-Wall Carbon Nanotubes in Alcohol Solvents. *J. Phys. Chem. B* **1999**, *103*, 4318–4322.
11. Clark, M. D.; Krishnamoorti, R. Dispersion of Functionalized Multiwalled Carbon Nanotubes. *J. Phys. Chem. C* **2009**, *113*, 20861–20868.
12. Ajayan, P. M.; Schadler, L. S.; Giannaris, C.; Rubio, A. Single-Walled Carbon Nanotube−Polymer Composites: Strength and Weakness. *Adv. Mater.* **2000**, *12*, 750–753.
13. Bourlinos, A. B.; Herrera, R.; Chalkias, N.; Jiang, D. D.; Zhang, Q.; Archer, L. A.; Giannelis, E. P. Surface-Functionalized Nanoparticles with Liquid-like Behavior. *Adv. Mater.* **2005**, *17*, 234–237.
14. Bourlinos, A. B.; Chowdhury, S. R.; Herrera, R. A.; Jiang, D. D.; Zhang, Q.; Archer, L. A.; Giannelis, E. P. Functionalized Nanostructures with Liquid-like Behavior: Expanding the Gallery of Available Nanostructures. *Adv. Funct. Mater.* **2005**, *15*, 1285–1290.
15. Rodriguez, R.; Herrera, R. A.; Archer, L. A.; Giannelis, E. P. Nanoscale Ionic Materials. *Adv. Mater.* **2008**, *20*, 4353–4358.
16. Warren, S. C.; Banholzer, M. J.; Slaughter, L. S.; Giannelis, E. P.; DiSalvo, F. J.; Wiesner, U. B. Generalized Route to Metal Nanoparticles with Liquid Behavior. *J. Am. Chem. Soc.* **2006**, *128*, 12074–12075.
17. Han, B. H.; Winnik, M. A. Luminescence Quenching of Dyes by Oxygen in Core−Shell Soft-Sphere Ionic Liquids. *Chem. Mater.* **2005**, *17*, 4001–4009.
18. Sun, L. F.; Fang, J.; Reed, J. C.; Estevez, L.; Bartnik, A. C.; Hyun, B. R.; Wise, F. W.; Malliaras, G. G.; Giannelis, E. P. Lead-Salt Quantum-Dot Ionic Liquids. *Small* **2010**, *6*, 638–641.
19. Lei, Y.; Xiong, C.; Dong, L.; Guo, H.; Su, X.; Yao, J.; You, Y.; Tian, D.; Shang, X. Ionic Liquid of Ultralong Carbon Nanotubes. *Small* **2007**, *3*, 1889–1893.
20. Li, Q.; Dong, L. J.; Deng, W.; Zhu, Q. M.; Liu, Y.; Xiong, C. X. Solvent-Free Fluids Based on Rhombohedral Nanoparticles of Calcium Carbonate. *J. Am. Chem. Soc.* **2009**, *131*, 9148–9149.
21. Bourlinos, A. B.; Stassinopoulos, A.; Anglos, D.; Herrera, R.; Anastasiadis, S. H.; Petridis, D.; Giannelis, E. P. Functionalized ZnO Nanoparticles with Liquidlike Behavior and their Photoluminescence Properties. *Small* **2006**, *2*, 513–516.
22. Agarwal, P.; Qi, H. B.; Archer, L. A. The Ages in a Self-Suspended Nanoparticle Liquid. *Nano Lett.* **2010**, *10*, 111–115.
23. Bourlinos, A. B.; Georgakilas, V.; Tzitzios, V.; Boukos, N.;

Herrera, R.; Giannelis, E. P. Functionalized Carbon Nanotubes: Synthesis of Meltable and Amphiphilic Derivatives. *Small* **2006**, *2*, 1188–1191.
24. Lei, Y.; Xiong, C.; Guo, H.; Yao, J.; Dong, L.; Su, X. Controlled Viscoelastic Carbon Nanotube Fluids. *J. Am. Chem. Soc.* **2008**, *130*, 3256–3257.
25. Mason, T. G.; Weitz, D. A. Linear Viscoelasticity of Colloidal Hard Sphere Suspensions near the Glass Transition. *Phys. Rev. Lett.* **1995**, *75*, 2770–2773.
26. Kegel, W. K.; van Blaaderen, A. Direct Observation of Dynamical Heterogeneities in Colloidal Hard-Sphere Suspensions. *Science* **2000**, *287*, 290–293.
27. Weeks, E. R.; Crocker, J. C.; Levitt, A. C.; Schofield, A.; Weitz, D. A. Three-Dimensional Direct Imaging of Structural Relaxation near the Colloidal Glass Transition. *Science* **2000**, *287*, 627–631.
28. Pusey, P. N.; van Megen, W. Observation of a Glass-Transition in Suspensions of Spherical Colloidal Particles. *Phys. Rev. Lett.* **1987**, *59*, 2083–2086.
29. Schall, P.; Weitz, D. A.; Spaepen, F. Structural Rearrangements that Govern Flow in Colloidal Glasses. *Science* **2007**, *318*, 1895–1899.
30. Petekidis, G.; Vlassopoulos, D.; Pusey, P. Yielding and Flow of Sheared Colloidal Glasses. *J. Phys.: Condens. Matter* **2004**, *16*, 3955–3964.
31. Podsiadlo, P.; Kaushik, A. K.; Arruda, E. M.; Waas, A. M.; Shim, B. S.; Xu, J. D.; Nandivada, H.; Pumplin, B. G.; Lahann, J.; Ramamoorthy, A.; Kotov, N. A. Ultrastrong and Stiff Layered Polymer Nanocomposites. *Science* **2007**, *318*, 80–83.